

Article

Performance Analysis of a Micro-Photovoltaic Concentrator Designed for Automotive Applications

Salima El Ayane ^{1,*}  and Ali Ahaitouf ^{1,2} 

¹ Laboratory of Intelligent Systems, Georesources and Renewable Energies, Faculty of Sciences and Technology, Sidi Mohamed Ben Abdellah University, Fez 30000, Morocco

² École Normale Supérieure de Fès, Sidi Mohamed Ben Abdellah University, Fez 30000, Morocco

* Correspondence: salima.elayane@usmba.ac.ma

Abstract: This research paper delves into the potential use of solar energy as an alternative energy source for future vehicles. The study introduces a system that overcomes the limitations of traditional solar panels by achieving a reduced thickness of less than 35 mm, while acknowledging the challenges faced by vehicles, such as the inability to maintain a fixed orientation towards the sun and frequent shading from surrounding objects. To tackle these challenges, our system incorporates the design of an asymmetrical and extended polynomial lens and optimizes it to widen the acceptance angle of incident sunlight, enabling the solar panels to capture a wider range of solar radiation, even when the vehicle is not ideally aligned with the sun. The goal of this innovative design is not only to maximize energy output in urban conditions, ensuring efficient solar utilization despite shading challenges, but also to maintain a compact, lightweight structure suitable for installation on vehicle rooftops and competitive with ordinary PV panels. Additionally, our system is a tracking and heat spreader-free structure. This simple structure enables cheaper mass production and the lightweight nature of the structure results in affordable manufacturing and assembly processes. Through collaboration with micro-fabrication, macro-electronic industries, and micro-LED technologies, our system is a strong candidate for a low-cost, high-efficiency system. The results show an optical efficiency of around 52.53% for incident rays at a 45° angle, with the remaining rays captured by adjacent lenses resulting in a total optical efficiency around 76%.

Keywords: micro-CPV; CO₂ emission; optical efficiency; solar-powered vehicle



Citation: El Ayane, S.; Ahaitouf, A. Performance Analysis of a Micro-Photovoltaic Concentrator Designed for Automotive Applications. *Energies* **2024**, *17*, 6470. <https://doi.org/10.3390/en17246470>

Academic Editor: Francesco Calise

Received: 7 November 2024

Revised: 9 December 2024

Accepted: 17 December 2024

Published: 23 December 2024



Copyright: © 2024 by the authors. Licensee MDPI, Basel, Switzerland. This article is an open access article distributed under the terms and conditions of the Creative Commons Attribution (CC BY) license (<https://creativecommons.org/licenses/by/4.0/>).

1. Introduction

Global efforts to combat climate change and reduce reliance on fossil fuels are driving the push for renewable energy and increased energy efficiency. Governments worldwide are supporting clean energy growth and promoting innovative practices to improve energy efficiency, particularly in the transportation industry, a major contributor to greenhouse gas emissions, with a 25% share. The shift towards electric vehicles (EVs) is a promising step, but for a meaningful reduction in emissions, the electricity powering EVs must come from cleaner energy sources. Solar energy, especially in countries with high sun radiation like Morocco, is being explored as a solution for powering EVs. Several automobile manufacturers have shown interest in using photovoltaics (PV) as an energy source for vehicles [1–6], with studies indicating potential energy savings and increased solar energy production [7–10]. Incorporating PV panels on car roofs has been shown to result in significant energy savings and reduced CO₂ emissions [11].

Nonetheless, achieving a significant reduction in greenhouse gas emissions is difficult due to the low efficiency of traditional flat PV panels and the space limitation of the vehicles (2.5 m² for the hood and roof) [12], leading many automotive manufacturers to abandon plans for solar-powered cars. To improve solar energy harvesting, increasing the efficiency of PV systems is necessary, with multi-junction solar cells showing promise. These cells

have a wide spectral sensitivity and can convert a large fraction of sunlight wavelengths. Efficiency milestones have been reached [13], with plans to produce even more efficient cells in the future [14,15]. While these cells are more expensive than silicon cells, concentrator photovoltaic technology allows for the use of smaller, high-efficiency cells. This technology uses optical systems to concentrate sunlight onto smaller solar cells, reducing the area needed for expensive multi-junction (MJ) cells while maintaining high power output [16].

Several studies have been conducted to study the applicability of this technology in the automotive sector [11,17,18]. Araki et al. [19] discussed the market potential of car roof PV installations and the suitability of static concentrator photovoltaic (CPV) systems for this application. Sato et al. [20] presented the design of a partial CPV module specifically designed for car roof applications. The system is based on a low-concentration static III-V/Si module that results in an annual efficiency of 27.3%. This efficiency allows for driving a distance of 27 km/day, assuming the best currently reported cell efficiency of the three-junction and Si cells. Despite the self-shading effect of the curved car roof, which causes non-uniformity in power generation. Also, the system presented reflection losses that also reduced the power generated by the system, resulting in a capability of collecting only 46.6% of the annual solar radiation incident on the car rooftop surface. Meanwhile, they used a hybrid structure with a Si solar cell incorporated that helps collect 36.4% of the annual incident solar radiation. This hybrid structure improved the power generation performance to match conventional Si PV systems. Vu et al. [21] emphasized the use of MJ solar cells with a flat CPV system to increase efficiency, noting the challenge of maintaining stability in vehicle structures due to sun-tracking mechanisms. Although their system shows a higher concentration ratio, and its suitability for high-DNI regions and employs an innovative structure based on spectrum splitting to improve performance. It acknowledges several limitations, including irradiance uniformity due to mirror usage and the need for additional features such as anti-reflection coatings that add more cost to the overall cost of the system, dependency on direct normal irradiance, and scalability challenges. Due to the complexity of the sun-tracking mechanism proposed, especially in automotive applications, space and design constraints are critical. Additionally, Vu et al. [22] introduced a static flexible concentrator photovoltaics module for electric vehicles, further exploring the potential of CPV systems in automotive applications. Vu et al. explore the use of the CPC as a concentrator. Although the system showed 25% annual efficiency, it still presents several limitations, namely the non-homogeneity of the irradiance and optical losses resulting from the TIR nature of the CPC concentrators. Although the CPCs present a wider acceptance angle than traditional lenses, they still require proper alignment with the sun for optimal performance (they perform poorly under cloudy or diffuse lighting conditions), which necessitates additional tracking mechanisms. Kenji et al. [23] calculated the minimum power conversion efficiency required for photovoltaic systems on car roofs to support the energy needs of electric vehicles, considering factors like vehicle mileage per kilowatt-hour of electricity. Furthermore, focus and efforts are going toward utilizing CPV systems for car roof applications, focusing on efficiency, standardization, and innovative design approaches to maximize solar energy utilization in electric vehicles. In this sense, micro-concentrator photovoltaics (MCPV) has been proposed as a promising alternative to leverage the technical achievements of CPV technology, while aiming to reduce costs by designing thinner modules with simplified manufacturing processes [24].

MCPV systems utilize smaller cells and optics compared to conventional CPV modules, with solar cell sizes less than a millimeter and concentrator optics a few centimeters thick [25–28]. This approach offers several advantages and addresses challenges faced by traditional CPV systems [27]. On the one hand, reducing the size of solar cells leads to lower heat input and temperatures, making thermal management easier without requiring external systems. Conductive interconnects help dissipate heat, and the lower total current received by each cell ensures that electrical performance is not greatly affected by any uneven flux distribution [29]. On the other hand, in this configuration, using full lenses instead of Fresnel lenses increases optical efficiency by omitting their draft angles or rip

rounding losses [28]. One last innovation MCPV brings is integrated tracking, which eliminates the need for bulky external structures [25,30,31]. All these make the MCPV system a suitable alternative for rooftop and car roof markets that were otherwise inaccessible with traditional CPV technology.

This research paper explores the potential application of solar power as an alternative energy source for future automobiles. The study introduces a system that addresses the limitations of traditional solar panels by achieving a reduced thickness of less than 20 mm. Recognizing the inherent challenges vehicles face, such as the inability to maintain a fixed orientation relative to the sun and the frequent shading from surrounding objects like buildings and trees, our proposed system is designed to cover all these factors.

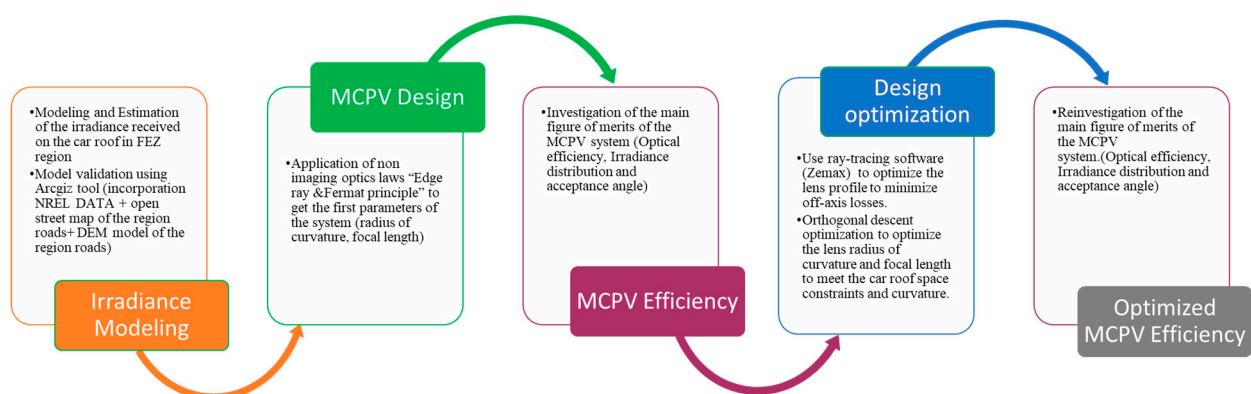
To overcome these obstacles, our system incorporates the design of an asymmetrical extended polynomial lens. This is different to traditional symmetrical lenses that struggle with variations in solar angles and irregular surface geometries, leading to inefficiencies in light capture. Our asymmetrical lenses offer tailored control over focal length and spot size, minimizing optical aberrations, ensuring precise control over the distribution of solar irradiance, improving energy capture efficiency.

The asymmetry also serves to expand the acceptance angle of incident sunlight, allowing the solar panels to capture a broader range of solar radiation even when the car is not ideally positioned relative to the sun.

Furthermore, a key aspect of our proposed system is its emphasis on maintaining a thin structure. We recognize the importance of reducing weight and ensuring aerodynamic efficiency in automobiles, which directly impacts their performance and energy consumption. Our system aligns with these objectives by enabling a compact, lightweight concentrator system (thickness of less than 20 mm) without sacrificing optical performance.

This paper is organized as follows: In Section 2, the methods and specifications are outlined, including the targeted cars and site of use, as well as the determination of solar irradiance. Section 3 provides a detailed description of the proposed MCPV system. Section 4 discusses the conducted simulation and the achieved results. Finally, Section 5 presents the conclusions drawn from the study.

Our research methodology and the organization of our paper are presented in Scheme 1.



Scheme 1. Flow chart illustrating the research methodology and the organization of the paper.

2. Methodology and Specifications

2.1. Targeted Car and Site of Use

In this research, a micro-photovoltaic concentrator was developed and optimized for a Dacia Spring vehicle, which is a city car manufactured by Dacia. The reason behind this car choice was firstly because the Dacia Spring is so affordable in comparison to other ones, and it is the most predominant car in the Moroccan market. Furthermore, the Dacia Spring features a spacious and level rooftop that is ideal for accommodating an MCPV system. The rooftop of the Dacia Spring measures 2.4 m². The Dacia Spring is equipped with lithium-ion batteries of 26.8 kWh, which allow the car to travel 8.3 km per kWh [32]. A

survey conducted to assess Moroccan attitudes towards electric cars found that the majority of the population relies on personal vehicles for daily commutes, with many traveling less than 30 km per day. By dividing 30 km (daily traveled distance) by 8.3 km/kWh, the vehicle would require 3.61 kWh of electricity per day, equivalent to an average of 1318 kWh/year annually. Furthermore, the study was performed in the Fez region (latitude: 33°59'58" N, longitude: 4°59'22" W, and altitude: 450 m). Fez, in northern Morocco, offers medium-to-high solar energy potential, with annual Global Horizontal Irradiance (GHI) averaging 5.5–6.0 kWh/m²/day and exceeding 7.0 kWh/m²/day in summer due to clear skies and optimal solar angles. Direct normal irradiance (DNI) is similarly robust, peaking at 7.0–8.0 kWh/m²/day during the summer months, making the region suitable for solar power systems, including concentrated photovoltaics. While Diffuse Horizontal Irradiance (DHI) is relatively low at 1.5–2.0 kWh/m²/day, Fez surpasses coastal areas and mountainous regions in solar potential, with fewer environmental challenges such as Sahara's sandstorms or coastal humidity. These conditions reduce system maintenance requirements, enhancing long-term performance and usability. Fez's hot, dry summers and abundant clear-sky days further solidify its viability for sustainable solar energy deployment.

In order to guarantee the effectiveness of our system, it is essential to achieve a high electricity conversion efficiency that is sufficiently high to support driving distances well beyond typical daily trips. To do so, first, we need to define the solar irradiance received on the car roof. However, as the car's orientation is not related to the position of the sun and the car roof is often shaded by the surrounding environment (buildings and trees), there is no direct relationship between the sun's direction and the direction of the panels. Thus, it is vital to redefine the incident angle of sunlight received by the car roof for an accurate design of the optic concentrators.

2.2. Solar Irradiance Determination

First, the hourly irradiance data for a full year in the Fez region of Morocco were obtained from the National Solar Radiation Database (NSRDB). For car roof applications, when designing an optical concentrator, it is important to consider diffused sunlight as there is no tracking system, unlike traditional concentrators.

However, to accurately calculate the irradiation on the car roof, the vehicle-specific environment must also be considered. Vehicles face challenges in maintaining a consistent orientation towards the sun due to their dynamic and independent orientation relative to the sun's position. Additionally, they are often shaded by surrounding objects while in motion or parked. As a result, a new model is needed to accurately estimate the amount of sunlight received by a vehicle roof, accounting for both the vehicle's specific operational environment and physical obstacles present in urban settings, which may lead to losses for both direct and diffuse components.

Since there is no correlation between the sun position and the car direction, it is further assumed that the diffuse irradiance is isotropic and depends only on the sky view factor, which represents the visible fraction of the sky. This dependency excludes factors like sun position, latitude, time of year, and street orientation. The irradiance losses can then be estimated based on the sky view factor, obstruction angle, and height–width ratio. In this study, we assumed an urban area close to obstructive sources such as buildings and trees, as depicted in Figure 1, assuming an infinite urban canyon with a specific orientation. For the sake of simplification, mean values were assumed for the height of buildings (h_{buil}), road width (d_{road}), vehicle width (d_{car}), and height (h_{car}). The following values were used: h_{buil} of 17.5 m and d_{road} of 15 m [12,33].

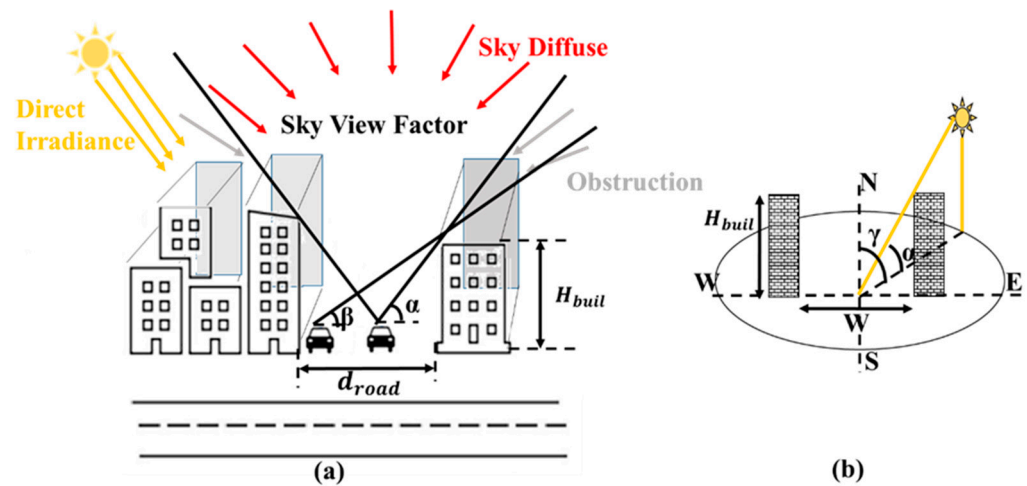


Figure 1. (a) The urban situation considered in this study, taking into account the obstruction angle for moving cars in the middle (α) and parked ones (β). (b) Obstruction angle definition and relationship with azimuth.

As presented in Figure 1, in the context of an infinitely long canyon, the obstruction angles for cars moving in the middle of the street (α) and those parked at the edge of the street (β) depend on the azimuth angle γ [34]. By applying trigonometric relationships, the obstruction angles for cars driving (in the middle of the street) (α) and those parked (at the edge of the street) (β) can be calculated as follows:

For moving cars,

$$\alpha = \tan^{-1} \frac{H_{buil}}{W/2\sqrt{(1 + \tan \gamma)}} \quad (1)$$

For parked cars,

$$\beta = \tan^{-1} \frac{H_{buil}}{W\sqrt{(1 + \tan \gamma)}} \quad (2)$$

The total diffuse irradiance I_D is the irradiance that would be received by a completely unobstructed horizontal surface. However, obstructions such as buildings or trees reduce the amount of diffuse light reaching the surface. This reduction can be quantified by the percentage loss (C) given by the following:

$$C = 1 - SVF \quad (3)$$

For moving cars,

$$SVF = \cos^2 \alpha_{avg} \quad (4)$$

α_{avg} is the average of the obstruction angle for cars in motion.

For parked cars, it will be as follows:

$$SVF = \frac{1}{2} \cos^2 \beta_{avg} \quad (5)$$

β_{avg} is the average of the obstruction angle of parked cars.

The actual diffuse irradiance received by the vehicle roof, $I_{d,car\ roof}$, can then be calculated as follows:

$$I_{d,car\ roof} = I_d \times SVF \quad (6)$$

On other hand, when it comes to direct irradiance, two key aspects have to be checked in order to analyze the reduction in the solar energy received by the vehicles and to assess the shading effect, whether they are in motion or parked. These key aspects are the sun's position in the sky and the orientation of the street in the city.

To assess the solar potential lost due to shading from the surrounding environment, we first had to assess the maximum solar energy available under ideal conditions. For this, we estimated the daily unobstructed horizontal irradiance $I_{B,Horizontal}$ as follows:

$$I_{B,Horizontal} = \int_{w_r}^{w_s} I_{B0} \times \cos \theta dw \quad (7)$$

I_{B0} represents the direct normal irradiance (DNI); w_r, w_s are the sunrise and sunset angles, respectively; and θ is the incident angle given by the following equation:

$$\cos \theta = \sin \delta \sin \varphi + \cos \delta \cos \varphi \cos w \quad (8)$$

φ is the latitude of the location, δ is the declination angle, and $w_{r,s}$ (sunrise and sunset angles, respectively) are calculated as follows:

$$w_{r,s} = \cos^{-1} \left(-\frac{\sin \delta \sin \varphi}{\cos \delta \cos \varphi} \right) \quad (9)$$

The daily irradiance for a canyon can be given by Equation (10), which incorporates sunrise and sunset angles (w_r, w_s , respectively), the incident angle (θ), and direct normal irradiance (DNI) denoted as I_{B0} .

Moreover, to ensure accuracy, this calculation filters irradiance to include only the periods when the sun's position exceeds the obstruction angle, derived from Equation (11). The obstruction angle (defined above in Equations (1) and (2)), determines the threshold beyond which sunlight is blocked. By applying this filter, the model accounts for only the usable, unobstructed solar irradiance.

$$I_B = \int_{w_r}^{w_s} f(w) \times I_{B0} \times \cos \theta dw \quad (10)$$

$$f(w) = \begin{cases} 1, & \text{if } \theta > \alpha \\ 0, & \text{otherwise} \end{cases} \quad (11)$$

The losses in the daily direct irradiance received by car roofs can be calculated as follows:

$$C = \frac{I_{B,H} - I_B}{I_{B,H}} \quad (12)$$

In our case, on the one hand, the resulting diffuse irradiance losses were about 60%, which means that 60% of the diffuse irradiance is not received by the car roofs because they are shaded by nearby obstacles (represented by an angle of around 50°) throughout the day. On the other hand, 22% of the direct irradiance was lost due to the obstruction of buildings. The resulting hourly values of solar radiation received by the moving cars' roofs are presented in the Figure 2. The figure illustrates a comparison of irradiance received on a vehicle's roof in an obstructed environment versus an unobstructed surface throughout the day on June 21 in Fez. The solid blue line shows the sunlight on the car roof with obstructions, while the dashed orange line represents the unobstructed sunlight. The shaded area between the two lines indicates the loss of sunlight due to obstacles like buildings and trees. The analysis demonstrates that sunlight losses are highest in the hours after sunrise and before sunset when the sun is low in the sky. During these times, obstructions create longer shadows, reducing the sunlight reaching the vehicle's roof. Conversely, around solar noon when the sun is highest in the sky, direct sunlight can reach the car's roof more easily, reducing the shading impact. However, even at peak hours, the sunlight on the vehicle is still lower than on an unobstructed surface, showing the ongoing influence of surrounding structures.

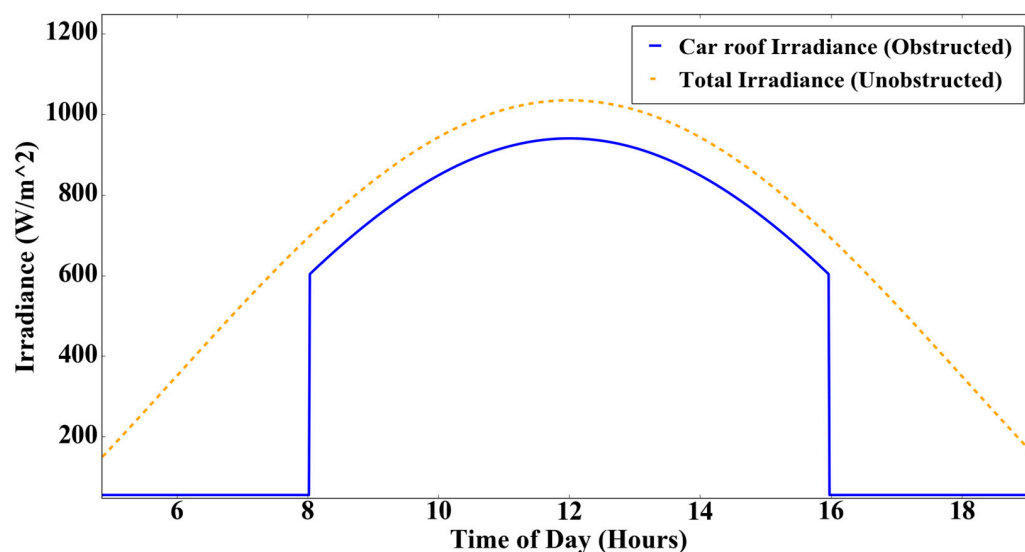


Figure 2. Comparison of irradiance on a vehicle's roof in an obstructed environment versus an unobstructed surface.

Furthermore, to validate the findings, theoretical annual calculations were compared to results from solar radiation analysis in ArcGIS Pro (V.3). First, the annual solar data of the region were obtained and extracted from NREL datasets. Then, the city map of the Fez region was obtained from Open Street Maps. Then, these data were clipped to specific areas, namely road networks and building zones, to identify the shaded regions accurately. Furthermore, the digital elevation model of the clipped area and ArcGIS area solar radiation model were used to analyze the city's solar energy potential, considering shadows from buildings and topography (see Figure 3). The calculated loss of 60% diffuse irradiance closely matched the ArcGIS results, confirming that areas with higher obstruction angles experienced greater reductions in solar radiation. This alignment between theoretical calculations and ArcGIS data enhances the reliability of the analysis, demonstrating the effectiveness of these calculations and data in quantifying shading losses. By combining these methods, we can improve the accuracy of solar energy assessments and make informed decisions about solar infrastructure placement in urban settings.

Figure 3 presents the distribution of solar radiation received by roads in Fez city. The map uses a color gradient to indicate varying levels of irradiance, with the darkest red areas representing the highest levels. These red-marked roads are likely wide streets with minimal shading, allowing for optimal exposure to sunlight throughout the day. The increased sunlight could be also linked to the alignment of the roads with the sun's path, maximizing solar exposure.

Areas with yellow shading (1060–1460) have moderate levels of solar radiation due to potential obstructions from nearby buildings or trees. Roads in this category may be affected by changes in the sun's position throughout the year or occasional shading from obstacles. Solar technology in these areas may be slightly less effective compared to the red zone. Blue and lighter shaded areas (450–1050) have progressively less exposure to sunlight, likely due to urban obstructions such as buildings. These streets are significantly impacted by shading from tall buildings or closely spaced urban structures. The lightest areas (below 450) receive minimal irradiance, indicating strong shading or less direct sunlight, possibly due to narrow streets or tall buildings obstructing sunlight.

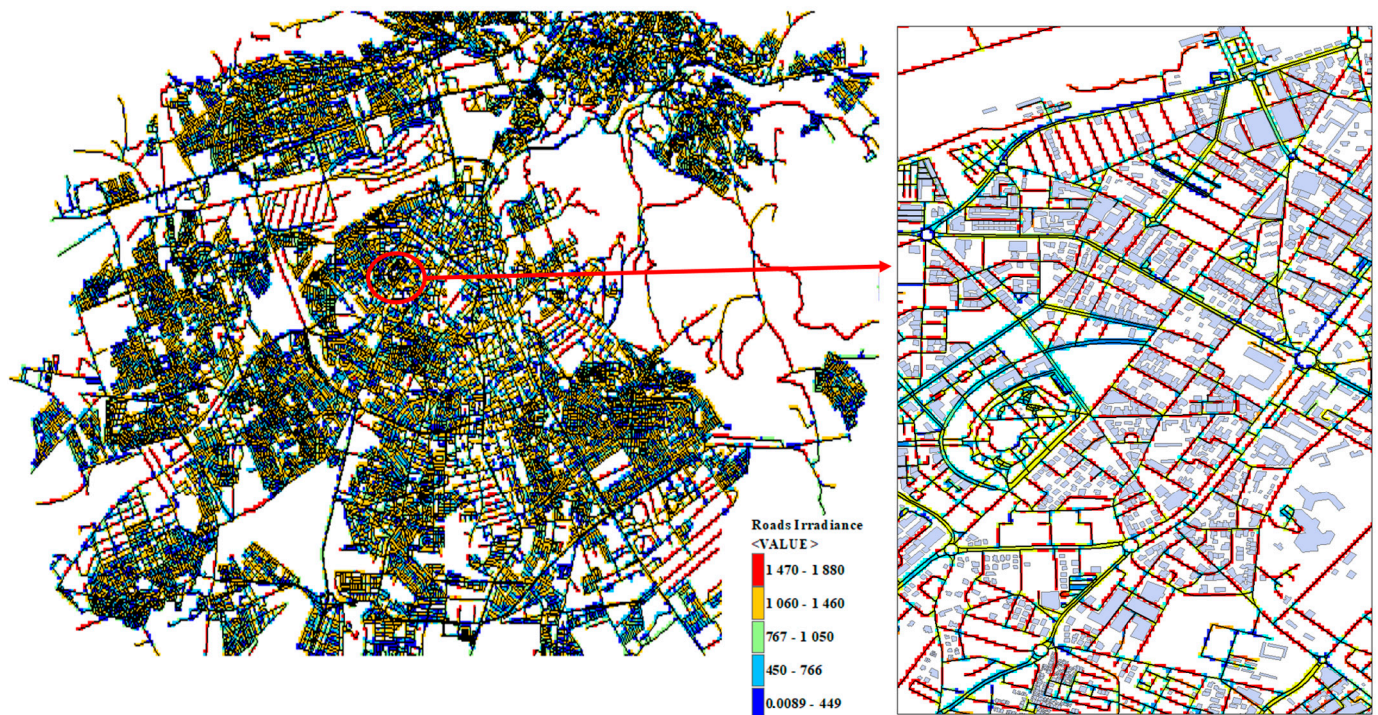


Figure 3. Spatial distribution of road irradiance in Fez: high solar potential on major roads and lower solar potential on small and dense ones.

2.3. Specifications

Once the solar irradiance captured by the car has been defined, to guarantee the effectiveness of the system, it is essential to have a high electricity conversion efficiency that can power the vehicle for longer distances than the average daily trip. A calculation of the trip distance dependency on the conversion efficiency was conducted to estimate the required conversion efficiency of the system. Our calculations assumed that an MCPV system with dimensions of $2\text{ m} \times 1.2\text{ m}$ was installed on a Dacia Spring car. Figure 4 illustrates the relationship between the trip distance and the conversion efficiency. The calculation was based on the following equations:

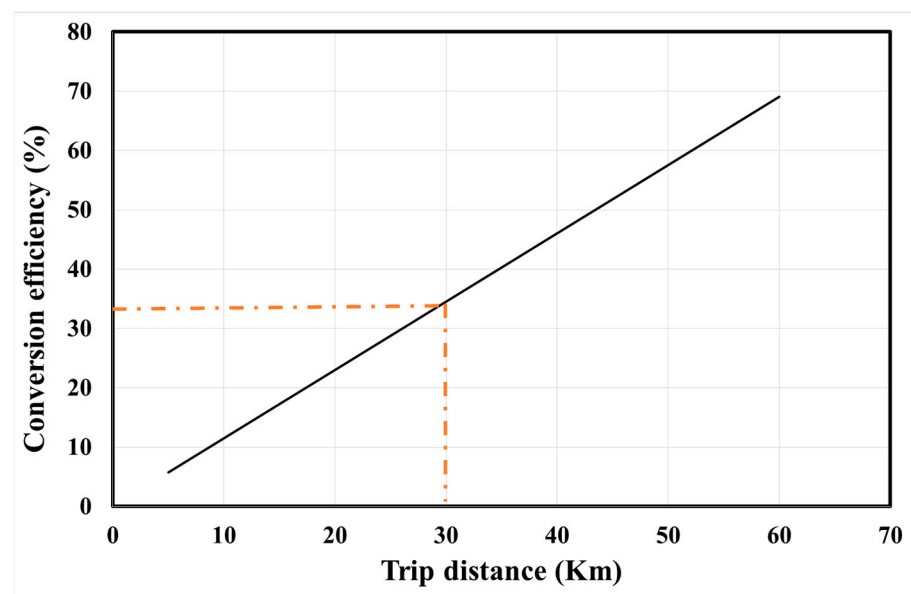


Figure 4. Variation in trip distance with conversion efficiency.

$$\text{Energy needed} = \frac{\text{Traveled distance}}{\text{Autonomy}} \quad (13)$$

$$\text{Solar energy collected} = \text{Surface} \times \text{mean Irradiance} \times \text{Insolation hours} \quad (14)$$

$$\text{conversion efficiency} = \frac{\text{available Energy}}{\text{Collected Solar energy}} \quad (15)$$

The conversion efficiency calculation results indicate that MCPV-powered vehicles equipped with a 34% efficiency module can travel an average of 30 km per day. This efficiency is achievable and promising. With the utilization of high-efficiency MCPV panels surpassing 34%, it becomes possible for the majority of households to power their cars with solar energy instead of relying on gasoline. This presents an exciting prospect for a cleaner and more sustainable society. One way to achieve this goal is by utilizing III-V cells, which have been demonstrated to be cost-effective while maintaining a high conversion efficiency. Furthermore, incorporating a concentrator can further reduce costs by decreasing the total cell area, making a static concentrator ideal for automotive applications. Concentrators with III-V cells provide various other benefits, including the ability to be mounted on a 3-D curved surface [35], which provides resistance to partial shading. In the next section, a detailed description of the proposed concentrator will be provided.

3. Proposed CPV System for Automotive Applications

In car rooftop applications, installing a tracker on a vehicle roof can be challenging. Therefore, a static concentrator is an excellent solution for automotive applications. Static concentrators with III-V cells provide numerous advantages [36], resistance to partial shading, and a potential improvement in aerodynamics by implementing suitable structures.

To be competitive, our module height should be minimized and within or less than the range of a typical PV flat panel, around 35 mm. For cost-effectiveness, plastic materials are preferred for mass production. Using plastic enables the lens array to be molded, reducing production costs. In our system design, the concentrator is based on a polymethyl methacrylate (PMMA) single lens. Additionally, given the moving nature of the car and the lack of correlation between the sun position and car direction, as well as the existence of potential obstructions on the road, the acceptance angle of our optical elements must be wide enough to intercept solar irradiance at shallow angles.

This study aimed to develop a photovoltaic concentrator system to cover the roof of a Dacia Spring car with dimensions of 2000 mm × 1200 mm × 35 mm. In order to keep the system thickness within 35 mm, the parameters of a single lens were selected with a lens size of $D = 10$ mm and a curvature radius of $r = 17.15$ mm. Moreover, the energy generation decreased as the concentration ratio increased due to the etendue law; for this, a concentration ratio of 10x was chosen for our system. What is more, since the module is to be mounted on a car roof, it is necessary to have a higher acceptance angle, and to ensure it has a larger cell for this, we opted for a three-junction solar cell of 3 mm. To achieve full coverage of the EV roof, a rectangular array of 200 × 120 lenses is required, using the chosen parameters for each individual lens. The different parameters of a single lens, namely the size of the lens D , the radius of curvature r , and the focal length, which is at the same time the thickness of the lens array, are presented in Figure 5.

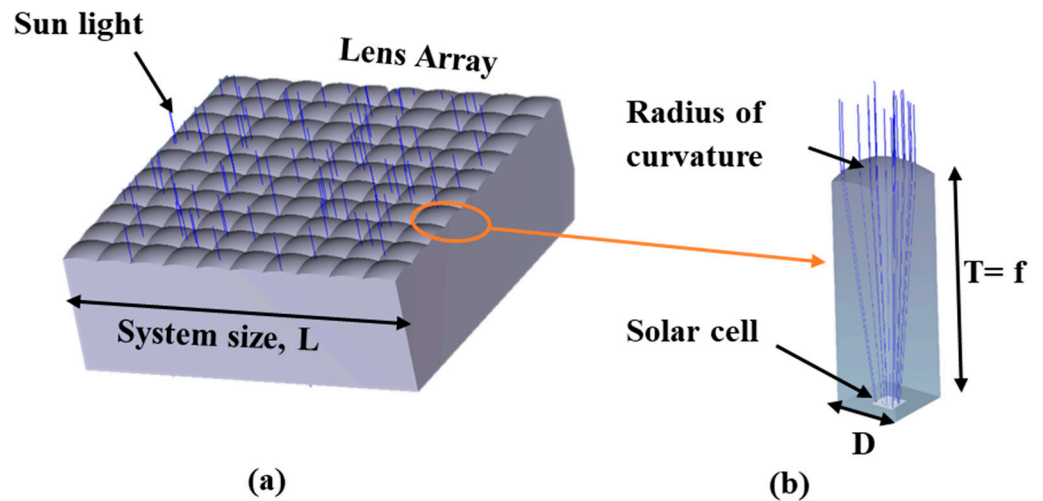


Figure 5. The micro-concentrator structure: (a) 3D view of the 10 × 10 lens array; (b) the details of one single lens.

The parameter values for the initial lens profile were achieved through the application of the edge ray principle where, for extreme rays, the Snell law will be expressed as below in Equation (16) (see Figure 6):

$$\sin(\theta) = n \sin r \tag{16}$$

$$\tan(r) = \frac{d}{2f} \text{ with } d = \frac{D}{\sqrt{C_g}} \text{ and } f_{\#} = \frac{f}{D} \tag{17}$$

$$\sin(\theta) = n \sin \left(\tan^{-1} \left(\frac{1}{2f_{\#} \sqrt{C_g}} \right) \right) \tag{18}$$

where C_g is the geometrical concentration ratio, n is the refractive index of the medium, $f_{\#}$ is the F-number of the lens, defined as the ratio between the focal lengths, d is the cell diameter, and D is the diameter of the lens.

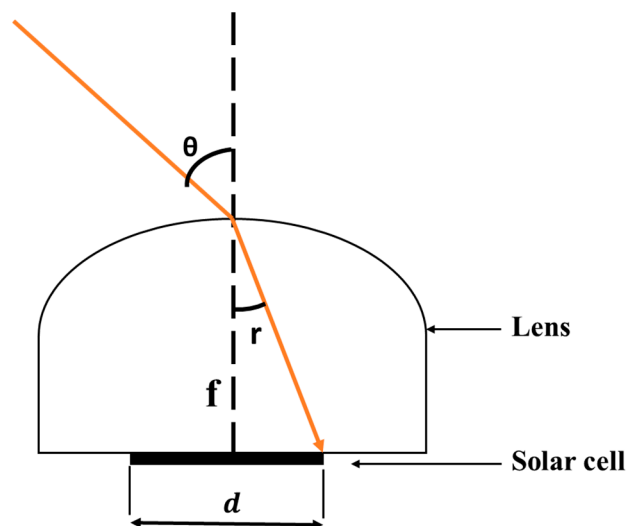


Figure 6. Edge ray applied to the design of the MCPV system.

4. Simulation and Results

While designing an optical system, three major criteria have to be taken into consideration. First is the optical efficiency η_{opt} that serves as a crucial measure of the system’s overall quality. It is defined as the ratio of light power at the concentrator output (receiver)

to the light power at its input. Another eminent feature of concentrators is the homogeneity of the concentrated light profile on the solar cell both spectrally and spatially. Non-uniform illumination leads to local overloaded current densities and efficiency losses due to the exceeded irradiation levels of some regions as well as increased series resistance [37]. Additionally, it might affect cell reliability due to thermal issues or limitations of the tunnel junction. The last figure of merit is the acceptance angle representing the system's tolerance to the misalignment between its optical axis and the axis of the incident solar radiation. The latter represents the ability of the system to capture higher incident angles; in our case, this incident angle gathers both direct and diffuse irradiance. This acceptance angle is generally defined as the incidence angle where the output power reduces to 90% of its maximum value (the optical efficiency measured at normal incidence 0°).

To assess the efficiency of our system, we considered the above-mentioned criteria with the aim of setting the optimal balance between maximizing the optical efficiency, ensuring the uniform distribution of the flux all over the cell surface, and achieving a wider acceptance angle.

Our system's modeling, design, and performance evaluation were carried out using Zemax Software (V.13). To achieve full coverage of the EV roof, a rectangular array of 200×120 lenses was required. However, for time saving and simplicity's sake, the simulation was performed on a 10×10 array with optical power detectors strategically positioned at the focused areas. The simulations were also based on the use of the irradiance data of the studied region in order to realistically model the efficiency of our system. Furthermore, the simulation accounted for various optical losses, such as Fresnel reflection losses and material absorption. However, certain losses that occur in real-world conditions, such as misalignment between optical elements, impurities in optical material, and degradation, were not accounted for in the simulation. These factors will be taken into consideration in future work when developing the prototype and conducting experiments.

Figure 7 demonstrates the impact of sunlight incident angles on optical efficiency through simulations conducted at angles ranging from 0° to 7° with 0.5° increments. The optical efficiency decreases as the sunlight direction increases. As the angle of incidence increases, the light rays tend to spread out more, making it challenging for the lens to effectively direct them onto the solar cell. In addition, the cosine law indicates that the quantity of light striking the surface diminishes in proportion to the cosine of the angle of incidence. This leads to a significant drop in optical efficiency at higher incident angles.

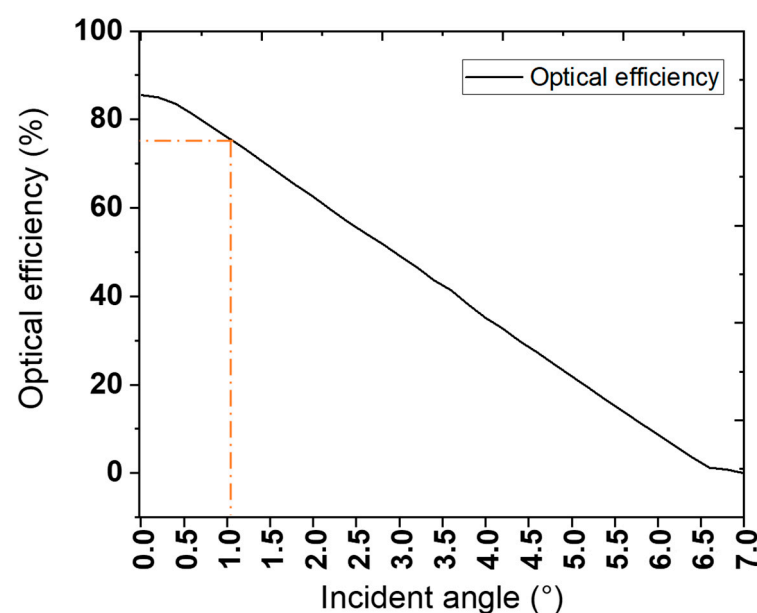


Figure 7. Variation in the optical efficiency of the micro-concentrator as a function of incremented incident angle (from 0° to 7° with 0.5°).

Our proposed system showed an optical efficiency of 85.53%, as demonstrated in Figure 7, which displays the simulated optical efficiency as a function of the incident angle. The results show that an increase in incident angle leads to a decrease in optical efficiency, as some sunrays are not captured by the optical system. Furthermore, the acceptance angle, which is defined as the angle at which the output power decreases to 90% of the optical power measured at normal incidence (0°), ($\theta_{90\%}$ is approximately 1° for our system).

Meanwhile, the irradiance distribution uniformity is generally determined in terms of variation in the value of a quantity Peak-to-Average Ratio, or PAR, which is defined as the maximum irradiance divided by the average irradiance of the cell surface. In our case, the PAR was around 1.2. The distribution of irradiance over the surface of the cell was non-uniform, as certain areas exhibited peaks while others had lower levels, as shown in Figure 8, where the irradiance distribution is presented.

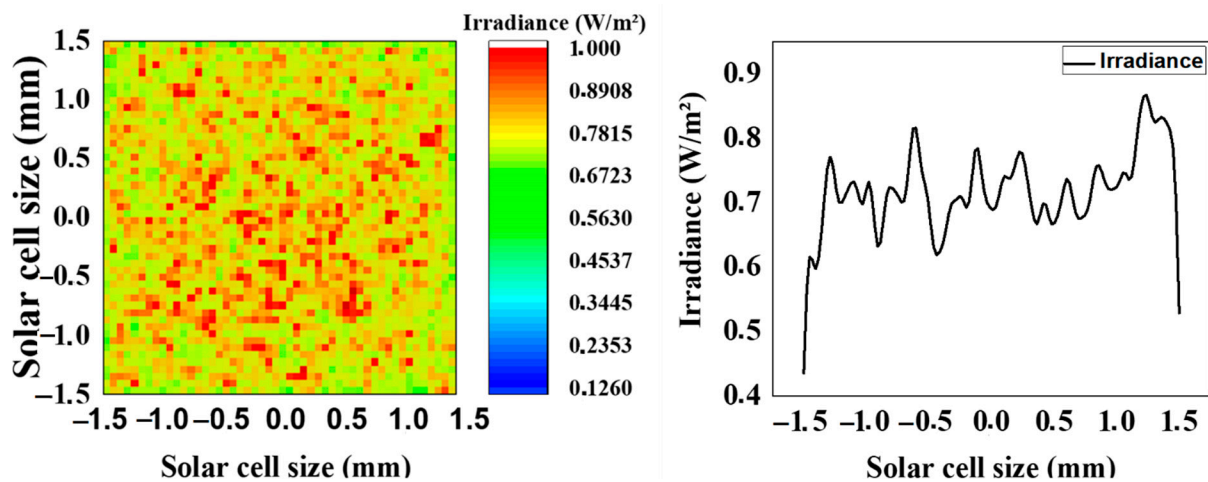


Figure 8. Irradiance distribution over the solar cell.

Our goal is to capture a wider beam of light and increase the acceptance angle of our system. Based on Equation (18), we suppose that our system accepts rays incident with $\theta = 45^\circ$. This value was chosen based on the fact that the studied region has a mean incident angle of around 34° ; therefore, we opted to construct a model with an incidence angle exceeding this value to ensure the reliable capture of higher incidence that may originate from any surrounding obstacles (diffused with higher incident angle). This was the aim of our optimization process where the radius of curvature and the focal length both were optimized in a way that our system's acceptance angle with 45° , also in a way that lost rays from the first cell are captured by the following one.

First, an extended polynomial was selected as one of the simplest asymmetrical lens equations to respond to our goal. Unlike conventional symmetrical lenses that face difficulties with changes in solar angles and irregular surface shapes, resulting in inefficiencies in light collection, our asymmetrical lenses provide customized control over focal length and spot size. This helps reduce optical aberrations and ensures precise management of solar irradiance distribution, enhancing energy capture efficiency. Furthermore, the asymmetry helps widen the acceptance angle of incoming sunlight, enabling solar panels to gather a wider spectrum of solar radiation, even when the vehicle is not optimally positioned in relation to the sun. Furthermore, the primary values of the lens curvature and focal length were optimized by the orthogonal descent method optimization algorithm provided by ray trace software.

Figure 9 presents a schematic view of the optimized lens. The optimization results in an extended polynomial lens with a radius of curvature of 8.1 mm and a shorter focal length in the range of 16 mm.

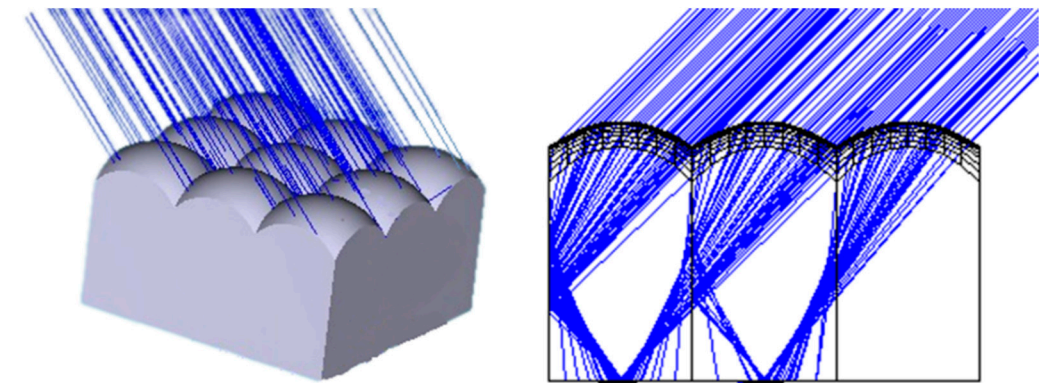


Figure 9. Optimized lens design that efficiently captures sunlight at low incident angles.

Figure 10 illustrates the optical efficiency of the optimized structure. The findings reveal that the optical efficiency of the first lens is in the range of 52.53% when the rays are incident with 45° ; this value is significantly lower than the one obtained before optimization. However, our structure ensures that the rays missed or not captured by the first lens are captured by the adjacent one. The adjacent lens in our simulation has an optical efficiency of around 24%, which results in a total optical efficiency of around 76%, only around 10% less than the on-axis efficiency obtained by the non-optimized lens, with a higher acceptance angle of around 45° .

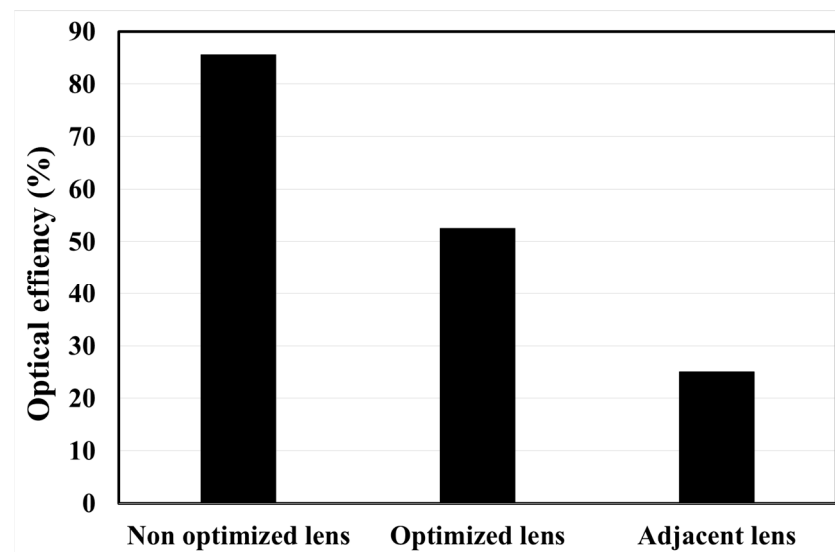


Figure 10. The optical efficiency obtained at a 45° incident angle with different lenses—the non-optimized lens, the optimized one, and the adjacent one—to check the rays missing from the optimized lens that were captured by the adjacent lens.

Our system demonstrated its potential by achieving an optical efficiency of approximately 52.5% at an incident angle of 45 degrees using only 3j solar cells, without the need for additional SI cells or hybridization. It is lightweight and utilizes smaller solar cells and optics, showcasing its promise compared to the existing literature. For example, Sato's work [20] achieved an optical efficiency of 46.6% with larger solar cells and optics, as well as a hybrid system incorporating SI solar cells to increase the efficiency to 27.3%. In comparison to flat concentrators like those presented by Vu et al. [21], which utilize MJ solar cells and a spectrum-splitting prism to achieve an electricity conversion efficiency of 32.88%, our system stands out for its efficiency and lightweight design. The flat CPV system presented by Vu et al. was bulky and heavy, with limitations such as irradiance

uniformity and the need for additional features like anti-reflection coating adding to the overall cost. Additionally, their sun-tracking mechanism was complex, particularly in applications with space and design constraints, such as automotive applications. Our system, on the other hand, offers a lightweight design, high efficiency, and does not require a complex sun-tracking mechanism. A prototype is all that is needed to test its efficiency under real-world conditions, showcasing its potential in comparison to flat concentrators and hybrid systems.

In terms of irradiance distribution, the special non-uniformity of illumination intensity on the cell's surface results in a non-uniform current density, i.e., the appearance of lateral currents between areas of high illumination and less enlightened ones. These lateral currents generate ohmic losses in series resistance, leading then to a decrease in the fill factor (FF) [37]. Figure 11a illustrates that the concentrated light is expanded at the focal plane at this incident angle. The figure shows that the irradiance distribution is not over the whole surface since it is broadened by the incident angle; it is not homogeneously distributed over the whole surface, and a hot spot was noticed around the cell side. The broadening of the concentrated light explains the dependency of the characteristics of the concentrated light, namely its shape, size, and position on the incident angle. Moreover, in Figure 11b, it can be noticed that the part of irradiance missed on the first lens was successfully captured by the adjacent one. Nevertheless, it is worth mentioning that the broadening of the acceptance angle is achieved at the cost of the on-axis performance (the optical efficiency as well as the uniformity of the irradiance distribution).

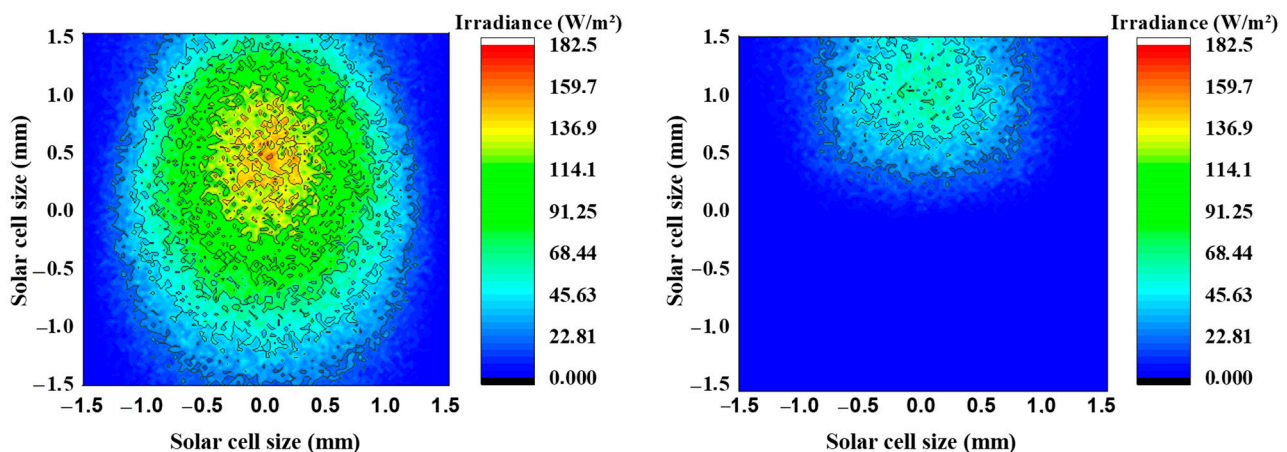


Figure 11. Irradiance distribution across the cell surface (a) and its adjacent cell (b) for the optimized structure.

Furthermore, the resulting structure of the system becomes thinner, which on the one hand makes it more competitive to flat ordinary PV panels, and on the other hand makes the lens manufacturing process easier as one can quickly mold it into the shape of the car roof. The most commonly used arrangement for high concentrators is a honeycomb for its closeness to a circular disk. Nevertheless, for our application, we opted for a grid arrangement, which is smoother than a honeycomb and can be easily assembled into the vehicle roof.

Overall, while our system shows promising results in terms of optical efficiency, lightweight design, and wide acceptance angle, it is crucial to validate its performance under real-world conditions. To achieve this, we are currently developing a prototype that will allow us to assess the system's effectiveness and reliability in practical settings. This validation process is essential to ensure that the system performs as expected in diverse, real-life scenarios.

5. Conclusions

This research paper explores the potential application of solar power as an alternative energy source for future automobiles. The study introduces a system that addresses the limitations of traditional solar panels by achieving a reduced thickness of less than 20 mm. Recognizing the inherent challenges faced by vehicles, such as the inability to maintain a fixed orientation relative to the sun and the frequent shading from surrounding objects like buildings and trees, our proposed system is designed in a way to cover all these factors.

To overcome these obstacles, our system incorporates the design of an asymmetrical extended polynomial lens. This lens serves to expand the acceptance angle of incident sunlight, allowing the solar panels to capture a broader range of solar radiation, even when the car is not ideally positioned relative to the sun.

Furthermore, a key aspect of our proposed system is its emphasis on maintaining a thin structure. We recognize the importance of reducing weight and ensuring aerodynamic efficiency in automobiles, which directly impacts their performance and energy consumption. By utilizing a slim design, our system aligns with these objectives while still maximizing solar energy conversion.

Overall, this research paper presents a comprehensive investigation into the feasibility of integrating solar power into future automobiles. Our proposed system addresses the challenges associated with orientation variability and shading, offering a solution that incorporates a specific lens design to expand the acceptance angle of sunlight and increase the energy yield. By maintaining a thin structure, our system aligns with the requirements of modern vehicles, aiming to pave the way for sustainable and energy-efficient transportation solutions.

While our system demonstrates promising results, several areas require further improvement. Specifically, the irradiance model needs revising to account for shading caused by trees and other urban features that cast shadows, as well as the reflected irradiance from surrounding buildings. Partial shading conditions, which are common in real-world environments, also need to be incorporated into the model. Additionally, the design of the whole module needs amending to enable it to fit inside a three-dimensional curved car roof surface.

A future study will focus on validating the structure under real-world conditions by developing a prototype of the system and conducting both indoor and outdoor tests.

Author Contributions: Conceptualization, methodology, investigation, writing—original draft preparation, S.E.A.; formal analysis; writing—review and editing, supervision, A.A. All authors have read and agreed to the published version of the manuscript.

Funding: This research received no external funding.

Data Availability Statement: The original contributions presented in the study are included in the article, further inquiries can be directed to the corresponding author.

Conflicts of Interest: The authors declare no conflicts of interest.

Nomenclature

C _g	Geometrical concentration ratio
CPV	Concentrator photovoltaics
d _{car}	Vehicle width
d _{road}	Road width
DNI	Direct normal irradiance
PV	Photovoltaics
EV	Electrical vehicles
h _{buil}	Height of buildings
h _{car}	Height
h _{tree}	Tree height
MCPV	Micro-concentrator photovoltaics

n_i	Refractive index of the incident ray
n_{POE}	Refractive index of the primary optical element
n_{SOE}	Refractive index of the secondary optical element
n_t	Refractive index of the transmitted (refracted) ray
PCB	Printed Circuit Board
PMMA	Polymethyl methacrylate
POE	Primary optical element
P_{out}	Absorption losses
PV	Photovoltaics
R_f	Fresnel losses
SC	Static concentrator
SOE	Secondary optical element
VIPV	Vehicle-integrated PV
$\theta_{(90\%)}$	Acceptance angle measured at 90% of the maximal
η_{opt}	Optical efficiency
η_{pp}	Conversion efficiency

References

1. Toyota Prius Toyota to Add Solar Panels to Some Prius Hybrids | Reuters. Available online: <https://www.reuters.com/article/us-toyota/toyota-to-add-solar-panels-to-some-prius-hybrids-idUST29871820080707/> (accessed on 16 September 2023).
2. Fisker Karma Targets Tesla with \$115,000 Solar-Boosted Hybrid | Automotive News. Available online: <https://www.autonews.com/article/20160811/OEM04/308119912/karma-targets-tesla-with-115-000-solar-boosted-hybrid> (accessed on 16 September 2023).
3. Sonata Hyundai Solar-Powered: 2020 Hyundai Sonata Hybrid Charges in the Sun. Available online: <https://www.autoweek.com/news/green-cars/a2144846/solar-powered-2020-hyundai-sonata-hybrid-charges-sun/> (accessed on 4 October 2023).
4. Motor Sono Solar on Every Vehicle | Sono Motors. Available online: <https://sonomotors.com/> (accessed on 18 September 2023).
5. Lightyear Long Range Solar Electric Vehicle—Lightyear 0. Available online: <https://lightyear.one/lightyear-0> (accessed on 19 September 2023).
6. Hanergy China’s Hanergy Unveils Four Solar-Powered Concept Cars-Autoevolution. Available online: <https://www.autoevolution.com/news/china-s-hanergy-unveils-four-solar-powered-concept-cars-109094.html> (accessed on 16 September 2023).
7. Araki, K.; Ota, Y.; Nishioka, K. Testing and Rating of Vehicle-Integrated Photovoltaics: Scientific Background. *Sol. Energy Mater. Sol. Cells* **2025**, *280*, 113241. [CrossRef]
8. Sierra, A.; Reinders, A. Designing Innovative Solutions for Solar-Powered Electric Mobility Applications. *Prog. Photovolt. Res. Appl.* **2021**, *29*, 802–818. [CrossRef]
9. Commault, B.; Duigou, T.; Maneval, V.; Gaume, J.; Chabuel, F.; Voroshazi, E. Overview and Perspectives for Vehicle-Integrated Photovoltaics. *Appl. Sci.* **2021**, *11*, 11598. [CrossRef]
10. Yamaguchi, M.; Masuda, T.; Araki, K.; Sato, D.; Lee, K.-H.; Kojima, N.; Takamoto, T.; Okumura, K.; Satou, A.; Yamada, K.; et al. Role of PV-Powered Vehicles in Low-Carbon Society and Some Approaches of High-Efficiency Solar Cell Modules for Cars. *Energy Power Eng.* **2020**, *12*, 375–395. [CrossRef]
11. Masuda, T.; Araki, K.; Okumura, K.; Urabe, S.; Kudo, Y.; Kimura, K.; Nakado, T.; Sato, A.; Yamaguchi, M. Static Concentrator Photovoltaics for Automotive Applications. *Sol. Energy* **2017**, *146*, 523–531. [CrossRef]
12. Dimensions, C. Car Dimensions of All Makes with Size Comparison Tools. Available online: <https://www.automobiledimension.com/> (accessed on 7 October 2023).
13. Geisz, J.F.; Steiner, M.A.; Schulte, K.L.; Young, M.; France, R.M.; Friedman, D.J. Six-Junction Concentrator Solar Cells. *AIP Conf. Proc.* **2018**, *2012*, 040004. [CrossRef]
14. Van Leest, R.H.; Fuhrmann, D.; Frey, A.; Meusel, M.; Siefer, G.; Reichmuth, S.K. Recent Progress of Multi-Junction Solar Cell Development for CPV Applications at AZUR SPACE. *AIP Conf. Proc.* **2019**, *2149*, 020007. [CrossRef]
15. Schube, J.; Höhn, O.; Schygulla, P.; Müller, R.; Jahn, M.; Mikolasch, G.; Steiner, M.; Predan, F.; Bartsch, J.; Dimroth, F.; et al. Mask and Plate: A Scalable Front Metallization with Low-Cost Potential for III–V-Based Tandem Solar Cells Enabling 31.6% Conversion Efficiency. *Sci. Rep.* **2023**, *13*, 15745. [CrossRef]
16. El Himer, S.; El Ayane, S.; El Yahyaoui, S.; Salvestrini, J.P.; Ahaitouf, A. Photovoltaic Concentration: Research and Development. *Energies* **2020**, *13*, 5721. [CrossRef]
17. Yamaguchi, M.; Masuda, T.; Araki, K.; Sato, D.; Lee, K.H.; Kojima, N.; Takamoto, T.; Okumura, K.; Satou, A.; Yamada, K.; et al. Development of High-Efficiency and Low-Cost Solar Cells for PV-Powered Vehicles Application. *Prog. Photovolt. Res. Appl.* **2021**, *29*, 684–693. [CrossRef]
18. Masuda, T.; Araki, K.; Okumura, K.; Urabe, S.; Kudo, Y.; Kimura, K.; Nakado, T.; Sato, A.; Yamaguchi, M. Next Environment-Friendly Cars: Application of Solar Power as Automobile Energy Source. In Proceedings of the 2017 IEEE 44th Photovoltaic Specialists Conference (PVSC), Washington, DC, USA, 25–30 June 2017; pp. 2076–2078. [CrossRef]

19. Araki, K.; Algora, C.; Siefer, G.; Nishioka, K.; Leutz, R.; Carter, S.; Wang, S.; Askins, S.; Ji, L.; Kelly, G. Standardization of the CPV and Car-Roof PV Technology in 2018-Where Are We Going to Go? *AIP Conf. Proc.* **2018**, *2012*, 070001. [[CrossRef](#)]
20. Sato, D.; Lee, K.H.; Araki, K.; Masuda, T.; Yamaguchi, M.; Yamada, N. Design of Low-Concentration Static III-V/Si Partial CPV Module with 27.3% Annual Efficiency for Car-Roof Application. *Prog. Photovolt. Res. Appl.* **2019**, *27*, 501–510. [[CrossRef](#)]
21. Vu, N.H.; Pham, T.T.; Shin, S. Flat Concentrator Photovoltaic System for Automotive Applications. *Sol. Energy* **2019**, *190*, 246–254. [[CrossRef](#)]
22. Vu, H.; Vu, N.H.; Shin, S. Static Concentrator Photovoltaics Module for Electric Vehicle Applications Based on Compound Parabolic Concentrator. *Energies* **2022**, *15*, 6951. [[CrossRef](#)]
23. Araki, K.; Ji, L.; Kelly, G.; Yamaguchi, M. To Do List for Research and Development and International Standardization to Achieve the Goal of Running a Majority of Electric Vehicles on Solar Energy. *Coatings* **2018**, *8*, 251. [[CrossRef](#)]
24. Ritou, A.; Voarino, P.; Raccurt, O. Does Micro-Scaling of CPV Modules Improve Efficiency? A Cell-to-Module Performance Analysis. *Sol. Energy* **2018**, *173*, 789–803. [[CrossRef](#)]
25. Ito, A.; Sato, D.; Yamada, N. Optical Design and Demonstration of Microtracking CPV Module with Bi-Convex Aspheric Lens Array. *Opt. Express* **2018**, *26*, A879. [[CrossRef](#)]
26. Voarino, P.; Ritou, A.; Seraine, C.; Roux, M.; Couderc, R. Microconcentration for Space Applications: A 7.6X TIR Design. *AIP Conf. Proc.* **2019**, *2149*, 050008. [[CrossRef](#)]
27. Domínguez, C.; Jost, N.; Askins, S.; Victoria, M.; Antón, I. A Review of the Promises and Challenges of Micro-Concentrator Photovoltaics. *AIP Conf. Proc.* **2017**, *1881*, 080003. [[CrossRef](#)]
28. Li, D.; Li, L.; Jared, B.; Keeler, G.; Miller, B.; Wood, M.; Hains, C.; Sweatt, W.; Paap, S.; Saavedra, M.; et al. Wafer Integrated Micro-Scale Concentrating Photovoltaics. *Prog. Photovolt. Res. Appl.* **2018**, *26*, 651–658. [[CrossRef](#)]
29. Li, G.; Xuan, Q.; Pei, G.; Su, Y.; Ji, J. Effect of Non-Uniform Illumination and Temperature Distribution on Concentrating Solar Cell—A Review. *Energy* **2018**, *144*, 1119–1136. [[CrossRef](#)]
30. Apostoleris, H.; Stefancich, M.; Chiesa, M. Tracking-Integrated Systems for Concentrating Photovoltaics. *Nat. Energy* **2016**, *1*, 16018. [[CrossRef](#)]
31. Price, J.S.; Grede, A.J.; Wang, B.; Lipski, M.V.; Fisher, B.; Lee, K.-T.; He, J.; Brulo, G.S.; Ma, X.; Burroughs, S.; et al. High-Concentration Planar Microtracking Photovoltaic System Exceeding 30% Efficiency. *Nat. Energy* **2017**, *2*, 17113. [[CrossRef](#)]
32. Dacia Spring. Nouvelle Dacia Spring Electric la Révolution Electrique de Dacia. 2021. Available online: <https://media.dacia.com/nouvelle-dacia-spring-electric-la-revolution-electrique-de-dacia-37729/> (accessed on 16 September 2023).
33. MATNUHPV. Ministère de l'Aménagement Du Territoire National, de l'Urbanisme, de l'Habitat et de La Politique de La Ville, NOUVEAU REGLEMENT D'AMENAGEMENT. Available online: <https://aust.ma/sites/default/files/2022-03/Nouveau%20re%CC%80glement%20d'ame%CC%81nagement.pdf> (accessed on 16 September 2023).
34. Brito, M.C.; Amaro e Silva, R.; Pera, D.; Costa, I.; Boutov, D. Effect of Urban Shadowing on the Potential of Solar-Powered Vehicles. *Prog. Photovolt. Res. Appl.* **2024**, *32*, 73–83. [[CrossRef](#)]
35. Sato, D.; Masuda, T.; Araki, K.; Yamaguchi, M.; Okumura, K.; Sato, A.; Tomizawa, R.; Yamada, N. Stretchable Micro-Scale Concentrator Photovoltaic Module with 15.4% Efficiency for Three-Dimensional Curved Surfaces. *Commun. Mater.* **2021**, *2*, 2–12. [[CrossRef](#)]
36. Araki, K.; Sato, D.; Masuda, T.; Lee, K.H.; Yamada, N.; Yamaguchi, M. Why and How Does Car-Roof PV Create 50 GW/Year of New Installations? Also, Why Is a Static CPV Suitable to This Application? *AIP Conf. Proc.* **2019**, *2149*, 050003.
37. Saura, J.M.; Chemisana, D.; Rodrigo, P.M.; Almonacid, F.M.; Fernández, E.F. Effect of Non-Uniformity on Concentrator Multi-Junction Solar Cells Equipped with Refractive Secondary Optics under Shading Conditions. *Energy* **2022**, *238*, 122044. [[CrossRef](#)]

Disclaimer/Publisher's Note: The statements, opinions and data contained in all publications are solely those of the individual author(s) and contributor(s) and not of MDPI and/or the editor(s). MDPI and/or the editor(s) disclaim responsibility for any injury to people or property resulting from any ideas, methods, instructions or products referred to in the content.